Nitroxide-Mediated Polymerization of Styrene Initiated from the Surface of Laponite Clay Platelets

C. Konn,[†,‡] F. Morel,[†,‡] E. Beyou,[‡] P. Chaumont,[‡] and E. Bourgeat-Lami*[,†]

Chimie, Catalyse, Polymère, Procédé, C2P2/LCPP, UMR 5265 CNRS/CPE/UCBL, Bât. 308F, BP 2077-43, Bd. Du 11 Nov. 1918, 69616 Villeurbanne Cedex, France, and IMP/LMPB, Laboratoire des Matériaux Polymères et Biomatériaux, UMR 5223 CNRS, Université Lyon 1-15, Bd. Latarget, 69622, Villeurbanne Cedex, France

Received February 1, 2007; Revised Manuscript Received June 19, 2007

ABSTRACT: Polystyrene chains were grown from the surface of synthetic Laponite clay platelets by nitroxide-mediated polymerization (NMP) of styrene using *N-tert*-butyl-*N*-[1-diethylphosphono-(2,2-dimethylpropyl)] (DEPN) as mediator. A novel water-soluble quaternary ammonium alkoxyamine was first synthesized and intercalated into the clay galleries by cation exchange. Polystyrene chains with controlled molecular weights and narrow polydispersities were then grown from the organoclay. The kinetics of styrene surface NMP polymerizations were investigated and compared with model polymerizations mediated by free alkoxyamine initiator molecules. Both reactions exhibited similar kinetics behaviors indicating that the clay platelets did not affect the livingness of polymerization. The PS-functionalized clay particles were colloidaly stable into toluene, a good solvent for polystyrene, and could be redispersed into tetrahydrofuran (THF) and a series of monomers after drying. Transmission electron microscopy (TEM) analysis of the films cast from the suspensions revealed a fully exfoliated structure of the clay tactoids within the polymer matrix.

Introduction

Because they often exhibit remarkable mechanical, thermal, optical, and flammability properties, polymer/clay nanocomposites have attracted considerable industrial and academic interest over the past few years.[1,2] In general, property enhancements originate from the nature of clay minerals, e.g., their small size and their high aspect ratios, and have been attributed to the large interface areas between the clay platelets and the host polymer matrix. However, as the silicate layers which compose primary clay particles are held together by electrostatic forces into stacky agglomerates, efforts must be done to separate the original clay stacks into individual layers and disperse them into polymers. To this purpose, various synthetic methods, such as exfoliation/adsorption, in-situ intercalative polymerization, and melt intercalation, have been reported. All these strategies require pretreatment of clay minerals in order to improve their compatibility with the host polymer and achieve a good dispersion. This can be realized for instance by treating the clay with silane coupling agents[3−5] or by replacing the interlayer metal cations by suitable organic compounds.[6] Ion exchange reactions with cationic surfactants including primary, tertiary, and quaternary ammonium ions or phosphonates render the silicate surface hydrophobic, which makes possible the subsequent intercalation of a variety of monomers and/or polymers. These organic cations can alternatively carry on one end a functional reactive group (e.g., a monomer or an initiator molecule) that can participate in the polymerization and promote exfoliation of the clay layers.[7] Following this direction, efforts have been done in the recent literature to grow polymer chains "from" clay surfaces by the so-called "grafting-from" technique using immobilized initiators.[8−11] Among the different methods, e.g., anionic,[9] cationic,[10] and anionic-coordinated ring-opening polymerizations,[11] controlled free radical polymerization (CRP) has attracted much attention due to its simplicity and versatility compared to ionic processes.[12] CRP not only enables to control the polymer chain length and length distribution but also offers the possibility to design grafted polymer chains with controlled architectures. CRP is usually divided into three categories: atom transfer radical polymerization (ATRP), reversible radical addition−fragmentation chain transfer (RAFT), and nitroxide-mediated polymerization (NMP). All three techniques have been used to build up highly dense polymer brushes from planar substrates[13] or nanoparticles,[14−18] including silica,[14] aluminum oxide,[15] iron oxide,[16] quantum dots,[17] and gold colloids.[18] Although there has been a great number of works in this field, comparatively only few works have been done on clay minerals so far.[19−29] In 1999, Sogah and co-workers demonstrated for the first time that polystyrene (PS) chains could be grown from the surface of Montmorillonite (MMT) by the NMP technique using a silicate-anchored initiator of the 2,2,6,6-tetramethylpiperidine *N*-oxide (TEMPO) derivative.[19] However, only limited information was provided in this preliminary communication. In a recent paper, they described the synthesis of poly(styrene-*b*-caprolactone) diblock copolymers using a multifunctional initiator anchored on the clay layers and capable to initiate simultaneously the ring-opening polymerization of ϵ-caprolactone and the NMP of styrene.[20] Further literature reports dealt with the ATRP technique and reported the successful intercalation of a variety of homopolymers[21−24] and block copolymers[25,26] into the interlamellar space of MMT or magadiite. Recently, increasing interest has also been devoted to the RAFT process as this method is applicable to a wide range of monomers and can be performed in a wide variety of solvents under a large range of conditions.[27−29]

In the present article, attention is given to the utilization of the NMP technique to grow PS chains from Laponite clay nanoparticles using the "grafting-from" approach. Laponite is a synthetic clay with well-defined dimensions and characteristics which makes it a good candidate for fundamental studies. To

* To whom correspondence should be addressed. E-mail: bourgeat@lcpp.cpe.fr.
† UMR 5265 CNRS-CPE-UCBL.
‡ UMR 5223 CNRS-Université Lyon 1.

10.1021/ma070283g CCC: $37.00
Published on Web 09/12/2007

the best of our knowledge, there has been only one report on the functionalization of Laponite particles using a surface-anchored initiator.[24b] In this article, a chlorosilane ATRP initiator was grafted to the edges of Laponite through sol−gel chemistry and used to initiate the growth reaction of poly(methyl methacrylate) chains. However, the results indicated that the polymerization was not controlled which may be attributed to undesirable interactions between the metal catalyst and the clay surface. Therefore, in an attempt to control the formation of polymer chains from the surface of Laponite, we have turned our attention to the NMP technique as this method does not rely on a metal catalyst. Moreover, the recent progress which has been done in the development of new alkoxyamine initiators now permits polymerizing a wide range of monomers by carefully selecting the appropriate control agent. The key reaction of NMP is an activation/deactivation process involving a reversible combination of propagating radicals with nitroxide free radicals:

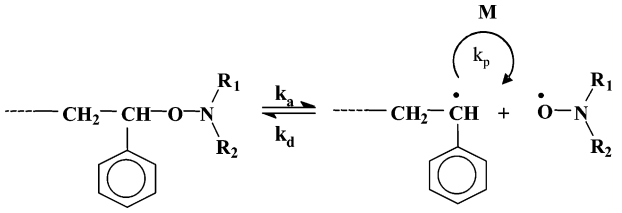

In order to apply the NMP technique to the functionalization of Laponite platelets, we designed a novel alkoxyamine initiator based on *N*-*tert*-butyl-*N*-[1-diethylphosphono-(2,2-dimethylpropyl)] (DEPN) and carrying a terminal quaternary ammonium functional group for anchoring to the clay layers. The synthetic strategy that we used in the present work is divided in two steps, as illustrated in Scheme 1. In order to produce nanoparticles with a high density of grafts, we first optimized the conditions for introducing the alkoxyamine initiator on the surface of the clay sheets. The NMP of styrene from the alkoxyamine-functionalized clay platelets was then examined in depth, and a correlation was established between the polymer chains grafting density and the initial concentration of the alkoxyamine initiator. Finally, dynamic light scattering (DLS) measurements and transmission electron microscopy (TEM) analysis were performed on the resulting materials in order to examine the effect of grafting on the degree of dispersion of the clay platelets both in suspension and in the polymer matrix.

Experimental Section

Materials. Laponite RD, with a cation exchange capacity (CEC) of 75 mequiv/100 g, was purchased from Rockwood Additives Ltd. (UK) and used as supplied. The water was purified using a Milli-Q Academic system (Millipore Corp.) (conductivity 18.2 μS and pH 6.8). Styrene (99%, Aldrich) and toluene (99.3%, Aldrich) were vacuum-distilled on a molecular sieve before use. DEPN (88%) was kindly supplied by Atofina and used as received. Tetrahydrofuran (99%, Acros), ethanol (95%, Acros), *p*-vinylchloromethylbenzene (90%, Acros), trimethylamine (24% aqueous solution, Acros), lithium bromide (99%, Acros), and *N*,*N*′-bis(3,5-di-*tert*-butylsalicylidene)-1,2-cyclohexanediaminato)manganese(III) chloride (Jacobsen catalyst, 98%, Acros) were used without further purifications. The sacrificial free initiator, a DEPN-based alkoxyamine (styryl-DEPN, Scheme 1), was prepared as described previously.[30]

Synthesis of the Quaternary Ammonium Alkoxyamine. The alkoxyamine **1** was synthesized following the procedure of Dao et al. (Scheme 2).[31] Typically, 16 g (0.11 mol) of chloromethylbenzene and 30.95 g (0.11 mol) of DEPN were dissolved in 600 mL of a toluene/ethanol mixture (50/50 (v/v)). The solution was introduced into a 1 L reactor purged with argon and heated to 90 °C. Then, 10 g (0.16 mol) of the Jacobsen catalyst, 8 g of the reducing agent $NaBH_4$, and 15.3 g (0.11 mol) of di-*tert*-butyl peroxide were added to the reactor, and the mixture was stirred for 2 days. The mixture was then evaporated to dryness and partitionated between dichloromethane (300 mL) and water (600 mL), and the aqueous layer was further extracted with dichloromethane (3 times 200 mL). The combined organic layers were then dried and evaporated to dryness. The crude product was purified on a column chromatography (carrier = heptane and heptane/ethyl acetate: 80/20), and the desired chloromethylalkoxyamine was obtained as a white solid (yield 7.5 g, 0.16 mol, 16%) and converted into a quaternary ammonium salt by reacting trimethylamine in diethyl ether. In a typical procedure, 3.0 g (6.7 mmol) of the chlorine-terminated alkoxyamine initiator was dissolved in 10 mL of Et_2O and mixed with 1.58 mL (6.7mmol) of a 24% aqueous triethylamine solution. The mixture was allowed to react at 20 °C overnight. The resulting precipitate was filtered off, and the solid residue was dissolved in 20 mL of toluene. The solvent was evaporated in vacuo and dried to give the salt **1** in 68% yield (2.3 g, 4.5 mmol). The alkoxyamine compound was characterized by FTIR and ^{1}H NMR. ^{1}H NMR: δ (ppm) = 0.9−1.6 (3s and 1t, 27H, CH_3), 2.4 (q, 4H, CH_2−O), 3.1−3.5 (s, 9H, N(CH_3)$_3$), 3.9 (m, 1H, CH−N), 4.65 (s, 2H, Ph−CH_2−N), 5.3 (q, 1H, CH−O−), 7 (m, 4H, ArH).

Intercalation of the Quaternary Ammonium Alkoxyamine (1) into Laponite. The incorporation of **1** into Laponite was performed by cation exchange. The reaction was carried out in deionized water at a clay solid concentration of 10 g L^{-1}. In a typical procedure, Laponite (1 g) was first suspended in water (50 mL) and magnetically stirred for 1 h to totally exfoliate the clay tactoids. Separate alkoxyamine solutions containing known amounts of **1**, comprised between 75 mg (0.16 mmol) and 943 mg (2 mmol), dissolved into 50 mL of water were added dropwise to the Laponite suspension.[32] These solutions were such as to cover a large range of concentrations from 20% up to 270% the CEC of Laponite. The mixtures were stirred for 4 h at room temperature. They were next centrifuged, and the supernatant solutions were analyzed by UV spectroscopy for determination of the equilibrium concentration of alkoxyamine in solution (C_e). The adsorbed amount was determined by difference between the total amount and the amount of free alkoxyamine and plotted as a function of C_e. This sorption isotherm was compared to that established by plotting the amount of intercalated cation determined by carbon elemental analysis of the clay powder after removal of physisorbed alkoxyamine molecules by extensive washing via a series of three centrifugations/redispersions in water followed by one cleaning in EtOH as follows:

$$\text{intercalated alkoxyamine (mmol g}^{-1}) = 10^3\Delta C/[1200Nc - \Delta CM] \quad (1)$$

where ΔC (wt %) stands for the difference between the carbon content of Laponite before and after cation exchange and M designates the molecular weight of the intercalated alkoxyamine molecule (M = 471.5 g mol^{-1}).

The powders were dried in vacuum at 30 °C and characterized by Fourier transform infrared (FTIR) spectroscopy and wide-angle X-ray diffraction (WAXS) before use. In the following, they will be referred to as Lap-*X*, where *X* corresponds to the amount of alkoxyamine introduced in the suspension expressed in percentage of the CEC.

NMP of Styrene from the Organoclay Surface. In a typical run, 0.16 g of the alkoxyamine-functionalized Laponite (surface alkoxyamine = 0.12 mmol), toluene (20 g, 0.2 mol), styrene (20 g, 0.19 mol), and the "free" alkoxyamine initiator (75 mg, 0.19 mmol) were introduced in a predried Schlenk flask. After stirring for a few minutes, the suspension was degassed by four freeze−pump−thaw cycles, and the polymerization mixture was heated to 110 °C for 32 h. The conversion was determined gravimetrically. The dry product (e.g., the PS-functionalized Laponite and the free PS chains) was redispersed into THF and characterized by transmis-

Scheme 1. Illustration of the Intercalation of the Quaternary Ammonium Alkoxyamine Initiator (1) into Laponite by Cation Exchange and the Subsequent Formation of Ionically Bonded Polystyrene Chains by Surface-Initiated NMP of Styrene Using a Sacrificial Alkoxyamine Initiator

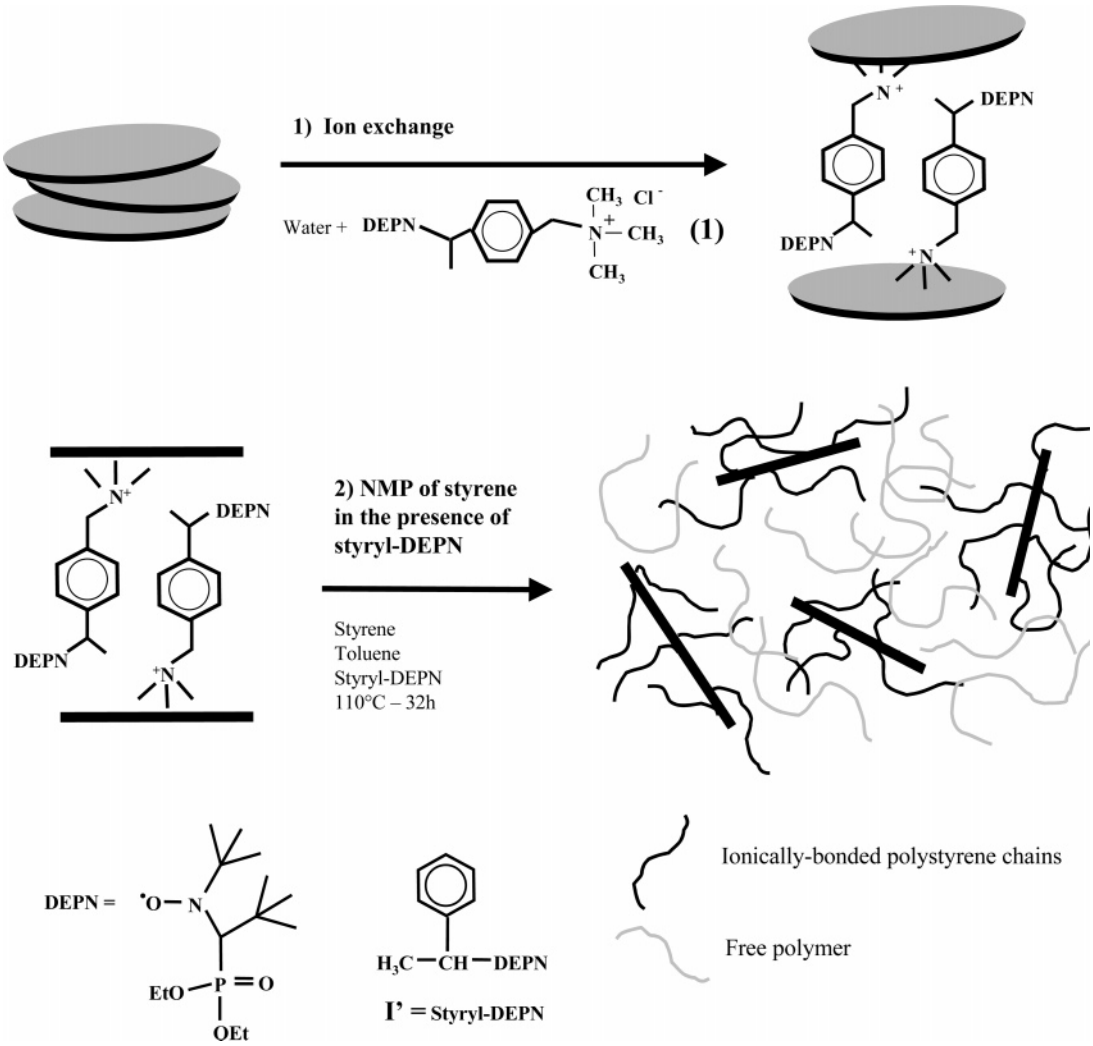

Scheme 2. Reaction Scheme for the Synthesis of the Quaternary Ammonium Alkoxyamine (1)

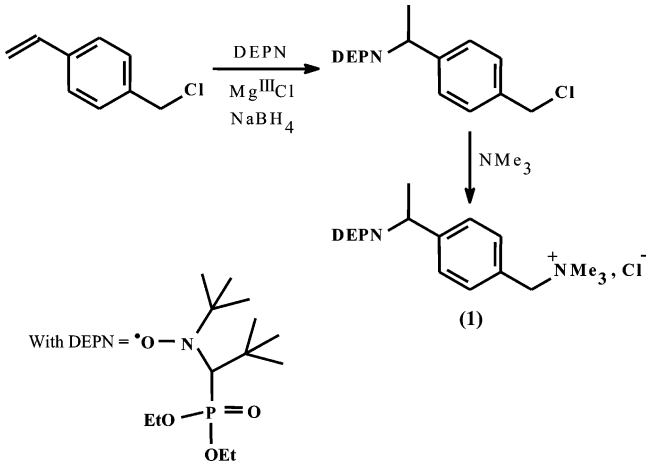

sion electron microscopy (TEM) and dynamic light scattering (DLS).

Recovery of Free and Tethered Polymer Chains. The free polymer was isolated from the grafted Laponite clay platelets by exhaustive cleaning of the suspensions by dialysis. In a typical example, 30 mL of the clay suspension was introduced into a cellulose membrane (Spectra/Por, MW cutoff, 1000) and repeatedly dialyzed against THF until no residual polymer could be detected in the recovered solution as attested by UV analysis. The free polymer solution and the PS-grafted Laponite suspension were dried at 60 °C to evaporate the solvant prior to characterization. The amount of intercalated polymer was determined by thermogravimetric analysis (TGA) of the PS-grafted Laponite powder using eq 2:

$$\text{intercalated amount (mmol/100 g)} = \frac{\left[\left(\frac{W_{25-500}}{100 - W_{25-500}}\right) \times 100 - W_{\text{Laponite}(25-500)}\right] \times 10^3}{M_n} \quad (2)$$

where W_{25-500} is the weight loss from 25 to 500 °C corresponding to the decomposition of polystyrene, M_n (g/mol) is its molar mass, and $W_{\text{Laponite}(25-500)}$ is the weight loss of Laponite determined before grafting.

Detachment of the ionically bonded polystyrene chains from the clay surface was performed as reported elsewhere.[20] Namely, 100 mg of the polymer-modified clay was suspended in 10 mL of THF. Then, 5 mg of LiBr was added to the suspension, and the mixture was refluxed under nitrogen overnight. The clay was decanted by centrifugation, and the polystyrene chains contained in the supernatant solution were precipitated out into a 10-fold excess of methanol yielding 80 mg of degrafted polymer. The number- and weight-average molecular weights of the free and grafted polymer chains were determined by size exclusion chromatography (SEC).

Characterizations. UV spectra were recorded on a Perkin-Elmer Lambda 35 UV/vis spectrometer calibrated with alkoxyamine

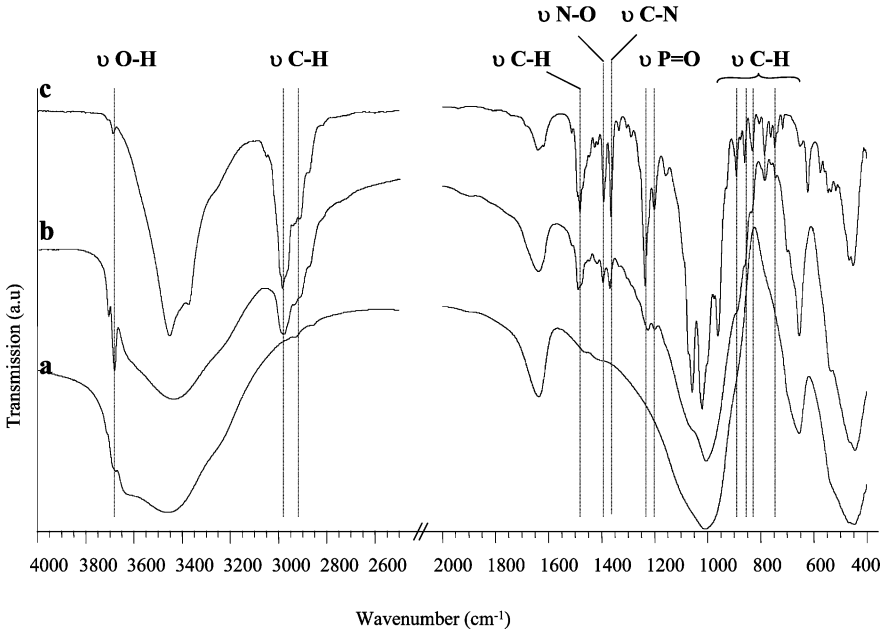

Figure 1. FT-IR spectra of (a) Na−Laponite, (b) the alkoxyamine-intercalated Laponite (Lap. 198), and (c) the quaternary ammonium alkoxyamine (**1**).

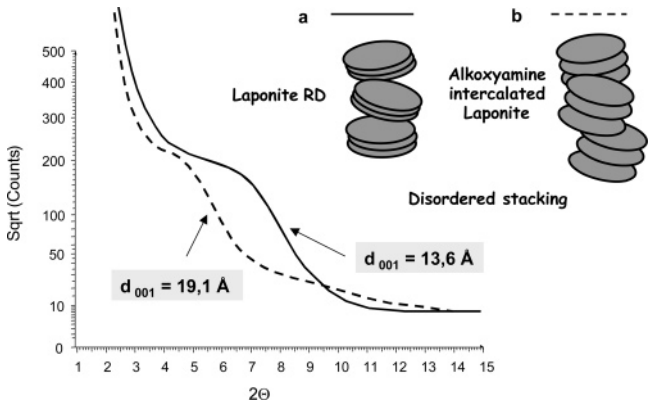

Figure 2. XRD patterns of (a) Na−Laponite and (b) the alkoxyamine-intercalated Laponite (Lap-198).

Table 1. Basal d_{001} Spacings Determined by XRD and Alkoxyamine Adsorbed Amounts Determined by UV and Carbon Elemental Analysis for Increasing Alkoxyamine Concentrations[a]

samples	alkoxyamine (% CEC)	exchanged amount (% CEC) EA	exchanged amount (% CEC) UV	exchanged amount (mequiv/100 g) EA	exchanged amount (mequiv/100 g) UV	d_{001} (Å)
Laponite	0	0	0	0	0	13.6
Lap-21	21	16	12	12	9	
Lap-43	43	44	39	33	29	
Lap-65	65	61	60	46	45	17.4
Lap-86	86	79	79	59	59	
Lap-107	107	87	88	65	66	18.7
Lap-198	198	91	148	68	111	19.1
Lap-269	269	96	160	72	120	

[a] Note that for elemental analysis and XRD measurements, the clay was extensively washed to remove physisorbed species.

solutions of known concentrations (range: 9.4×10^{-6}−9.4×10^{-5} M). FTIR spectra were recorded on a Nicolet FTIR 460 spectrometer using powder-pressed KBr pellets. Specimens for the measurements were prepared by mixing 2 mg of the sample powder with 100 mg of KBr and pressing the mixture into pellets. FTIR spectra were obtained at a resolution of 4.0 cm^{-1} at room temperature in a wavenumber range between 4000 and 400 cm^{-1} and averaged

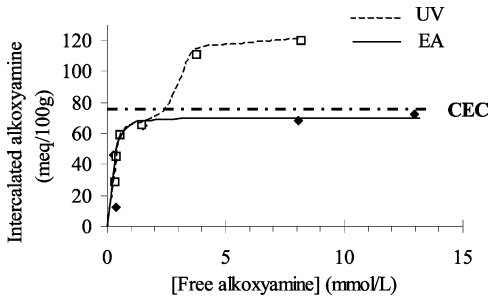

Figure 3. Alkoxyamine adsorbed amounts determined by UV analysis of the serums and carbon elemental analysis of the organoclay as a function of the quaternary alkoxyamine equilibrium concentration. For elemental analysis, the clay was washed with water in order to remove physisorbed species.

over 200 scans. The powder X-ray diffraction (XRD) measurements were performed on a Siemens D500 diffractometer (Ni-filtered Cu Kα radiation, $\lambda = 1.5405$ Å). The d_{001} basal spacings were calculated from the 2θ values using the EVA software. TGA was carried out with a Mettler TG 50/TA 3000 thermobalance, controlled by a TC10A microprocessor. Samples were heated at 10 °C/min under a nitrogen flow (150 mL/min). SEC analysis were performed at 45 °C using a Waters SEC device equipped with a 410 Waters differential refractometer, a 996 Waters photodiode array detector, a 717 Waters autosampler, a 515 Waters HPLC pump, and a set of two Waters microstyragel columns (HR1 and HR4; weight range: 5000−600 000 g/mol). THF was used as eluent at the flow rate of 1 mL min^{-1}. Polymer molecular weights were derived from a calibration curve based on polystyrene standards. Particle size was determined by DLS at 670 nm using a Malvern autosizer Lo-c apparatus with a detection angle of 90°. The measurements were carried at 23 °C on highly diluted samples in order to rule out interaction and multiple scattering effects. The intensity average diameter was computed from the intensity autocorrelation data using the cumulant analysis method.[33] Films were formed by allowing a suspension to dry in air. Specimens for TEM analysis were prepared by cryosectioning the samples at 20 °C using a Leica EM-FCS ultramicrotome. The ultrathin sections (∼60 nm thick) were placed on copper TEM grids and imaged using a Philips CM120 electron microscope operating at 80 kV.

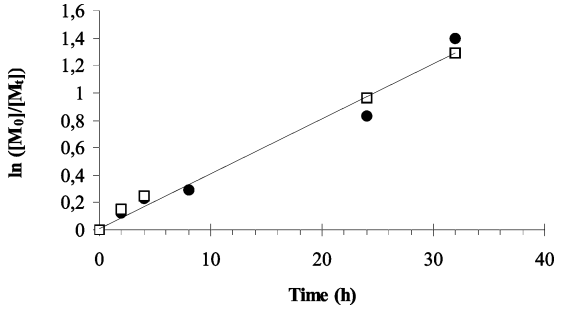

Figure 4. Plots of $\ln([M_0]/[M_t])$ vs time for the solution polymerization of styrene (50% in toluene) at 110 °C in the absence (□) and in the presence (●) of Laponite. The clay used in this experiment is Lap-269; [styrene]/[initiator] = 625.

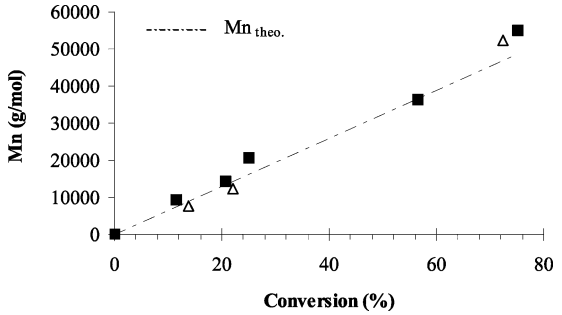

Figure 5. Evolution of M_n determined by SEC as a function of the monomer conversion for the solution polymerization of styrene (50 wt %) in toluene at 110 °C in the absence (△) and in the presence (■) of Laponite. The clay used in this experiment is Lap-269; [styrene]/[initiator] = 625.

Results and Discussion

Intercalation of the Quaternary Ammonium Alkoxyamine into Laponite. The clay used in the present work is Laponite RD. Laponite is a synthetic trioctahedral 2:1 layered silicate structurally related to the naturally occurring hectorite but free from the extraneous elements which are normally present in samples of that mineral. Laponite consists of disk-shaped particles of about 30 nm in diameter and 0.96 nm in thickness.[34] It has a layer structure composed of repeats of six octahedral magnesium ions sandwiched between two layers of four tetrahedral silicon atoms. Isomorphous substitution of magnesium with lithium in the central sheet creates a net negative charge compensated by intralayer sodium ions located between adjacent layers in a stack. In aqueous solutions, water molecules are intercalated into the interlamellar space of Laponite, leading to an expansion of the mineral due to the hydration of the metal ions. The latter can be thus replaced by other cations by simple ion exchange reactions. The cation exchange capacity of Laponite is 75 mequiv/100 g.[35] Evidence of exchange of the sodium ions by the quaternary ammonium alkoxyamine **1** was provided by FTIR analysis. Figure 1 compares the FTIR spectra of Laponite before and after ion exchange with that of the alkoxyamine molecule. Characteristic vibrations of the phosphate ($\nu_{P=O}$, 1225 and 1199), the nitroxide (ν_{N-O}, 1395), the cyanide (ν_{C-N}, 1369), the styrenic (ν_{CH}, 740−900 cm^{-1}), and the aliphatic (ν_{CH}, 2800−3000 cm^{-1}; δ_{CH}, 1350 cm^{-1}) groups of the alkoxyamine compound clearly attest for the presence of **1** on the clay surface. Moreover, the FTIR spectrum of the hydroxyl region of Laponite exhibits a strong and wide OH stretching vibration band in the range 3600−3100 cm^{-1} due to physisorbed water and hydrogen-bonded silanol groups and a shoulder at 3687 cm^{-1} corresponding to terminal nonreacted MgOH.

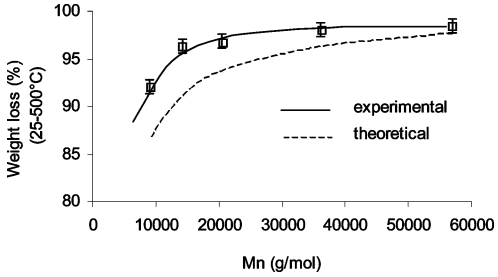

Figure 6. Evolution of the experimental and of the theoretical weight losses determined by TGA as a function of the molecular weight of the grafted polystyrene chains determined by SEC. The theoretical values are calculated on the basis of a surface density of 72 mequiv/100 g assuming 100% initiation efficiency.

The X-ray diffraction patterns of Na−Laponite and ion-exchanged Laponite are plotted in Figure 2. A broad peak centered around $2\theta = 6.5°$ ($d_{001} = 13.6$ Å) attributable to a low degree of ordering is observed for Laponite RD. The difficulty in observing a sharp diffraction peak in this case is due to the very small dimensions of the clay platelets which prohibit long-range organization. The diffraction peak was shifted to a lower angle after ion exchange, indicating an increase of the interlayer distance of the clay sheets of 5.5 Å for the highest alkoxyamine concentration. The alkoxyamine concentration dependences of the d_{001} values are listed in Table 1. The gradual variation of the basal spacings as a function of the amount of alkoxyamine is in agreement with previous findings in the literature.[34a,b,36−39] Indeed, stepwise changes in basal spacings have been reported for instance during the addition of increasing amounts of long chain cations such as dimethyldioctadecylammonium,[37] cetylpyridinium,[38] or cetyltrimethylammonium[39] to MMT. The authors observed interlayer separation values of 4 and 8 Å for low organic loadings which were attributed respectively to the formation of single- and double-layer complexes, with the alkyl chains being oriented parallel to the clay sheets. Herein, the XRD data of Table 1 indicate a gap of ∼9.5 Å between the clay layers for the Lap-198 sample after substraction of the intrisic thickness of a Laponite platelet (e.g., 9.6 Å). This interlamellar spacing is of the same order of magnitude as that reported in the literature for the intercalation of a series of alkylammonium salts into Laponite.[40,41] Although such a moderate spacing is consistent with the quaternary ammonium salt lying flat on the clay surface given the bulky DEPN moiety, it could also correspond to the alkoxyamine molecules being oriented nearly perpendiculary to the clay sheets as the end-to-end distance of **1** in a fully extended conformation can be estimated to be around 11 Å. Previous authors have also suggested that intercalated alkylammonium surfactants could stand at a certain angle to the silicate surface which situation is intermediate between the planar and the vertical configurations. Such a scenario could also apply to the present system although further investigations would be necessary to descriminate between the different possibilities and definitely conclude on this point. Such in-depth investigations are beyond the scope of this article.

Quantitative data were obtained by carbon elemental analysis of the organically modified Laponite and by UV analyses of the serums. The results are listed in Table 1 and plotted in Figure 3 as a function of the residual concentration of alkoxyamine in solution (so-called "free" alkoxyamine). The results of UV analysis clearly show an isotherm pattern. The exchanged amount increases almost linearly at low alkoxyamine contents and then reaches a pseudo-plateau at nearly 100% of the CEC followed by a further increase up to values corresponding to

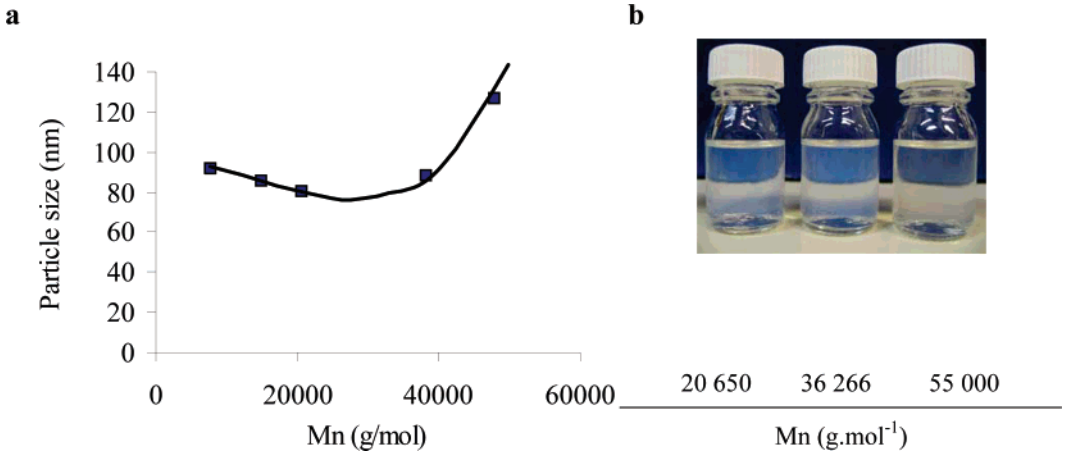

Figure 7. (a) DLS hydrodynamic diameters of the polystyrene-grafted Laponite particles as a function of the molecular weight of the grafted polystyrene chains determined by SEC (the line is to guide the eye) and (b) suspensions of the PS-grafted Laponite in THF at 2 wt % loadings.

Table 2. SEC Analysis of the Grafted and Free Polystyrene Chains, Grafting Densities, and DLS Hydrodynamic Diameter of Polystyrene-Functionalized Laponite Particles as a Function of Time

				free polymer in solution		surface-grafted polymer				
samples	reaction time (h)	conv (%)	$M_{n,th}$ (g/mol)[b]	M_n (g/mol)	M_w/M_n	M_n (g/mol)	M_w/M_n	weight loss (%)[c]	tethered polymer[d]	particles diam (nm)[e]
1	2	11.6	7 550	9 190	1.50			92.0	125	92.0
2	4	20.7	13 440	14 260	1.38	12 300	1.3	96.2	177	85.7
3	8	25.0	16 220	20 650	1.28	13 500	1.3	96.7	142	80.2
4	24	56.6	36 500	36 266	1.25	27 500	1.25	98.0	135	88.5
5	32	75.2	48 800	55 000	1.50	56 900	1.51	98.4	108	127.3

[a] Initiator = surface-grafted initiator + free initiator. The intercalated alkoxyamine concentration is equal to 72 mmol/100 g of Laponite, and that of the free initiator is equal to 94 mmol/100 g. [b] $M_{n,th} = ([M]_0/[I]_0) \times M_w$ of styrene $\times$ conv)/100. [c] Determined by thermogravimetric analysis in the range 25−500 °C. [d] In mmol/100 g, calculated using eq 2. [e] Determined by dynamic light scattering in THF.

nearly 2 times the CEC. Zhang et al. have shown that the adsorption of quaternary amines on montmorillonite occurs in three steps: (i) a cation exchange reaction, (ii) adsorption of ion pairs, and (iii) tail−tail interactions.[42] The fact that the adsorbed amount increases to values higher than the CEC is consistent with a stepwise adsorption. The first step is generally attributed to the neutralization of the anionic clay sites through cation exchange while further steps correspond to the progressive intercalation of multilayers of surfactants. As far as alkylammonium salts are concerned, molecular adsorption has been reported to occur through ionpairs formation and van der Waals interactions between adjacent alkyl chains.[36] In the present system physisorption may proceed rather through $\pi-\pi$ interactions of the aromatic ring of the alkoxyamine compound or by hydrogen bonding between the phosphonic ester moiety of **1** and the OH groups located at the edges of the Laponite platelets. A similar adsorption scenario was put forward in the case of silica grafted with a DEPN-based alkoxyamine initiator carrying triethoxysilyl end groups.[43] Unlike UV analysis, the carbon elemental analysis data after washing of the clay powder indicate an increase of the amount of alkoxyamine interacting with Laponite up to a plateau corresponding to the CEC as expected for full exchange. As the UV and elemental analysis data are consistent in the low alkoxyamine concentration region, this suggests that physisorption occurs only for high concentrations when all exchanged sites have been used. In summary, the above data reveal the occurrence of two phenomena: an ion exchange reaction for low alkoxyamine concentrations and molecular adsorption for higher concentrations. In the following, care will be taken to remove physisorbed alkoxyamine molecules by exhaustive cleaning before performing the polymerization reaction in order to avoid growing of polymer chains from initiating groups which are not tightly bonded to the clay layers. Carbon elemental analysis will be used to determine with accuracy the amount of ionically bonded alkoxyamine after extensive washing of adsorbed molecules.

NMP of Styrene from the Functionalized Clay Surface. Based on previous works in the literature,[14f] and as mentioned earlier, the polymerization was performed in the presence of a known amount of "free" sacrificial initiator. The addition of "free" alkoxyamine creates an overall concentration of nitroxide in the polymerization mixture, which controls the chain growth of both the immobilized and soluble initiators, and allows one to achieve a good molecular weight control. Figure 4 shows the evolution of $\ln([M_0]/[M_t])$ vs time for a model polymerization reaction mediated by free alkoxyamine initiator molecules and a polymerization initiated from the surface of Laponite functionalized at 269% the CEC (sample Lap-269 in Table 1). The linear relationship indicates that the first-order kinetics typical of polymerizations mediated by stable free radicals also applies to the present system. In addition, the fact that both polymerizations exhibit similar rate constants proves that the polymerization is not affected by the presence of the clay platelets. In Figure 5, the polymer number-average molecular weights are plotted against the conversion. It can be seen that the experimental values agree well with the theoretical ones as expected for a controlled polymerization.

To go a step forward, we compared the molecular weights and the polydispersity indices of the electrostatically bonded and the free polymer chains. Table 2 indicates a relatively good agreement between the two sets of data as already reported in the literature for the grafting of inorganic particles by controlled radical polymerization.[13c,24b] However, in both cases polydispersity indices (PDI) are quite high, suggesting that the control

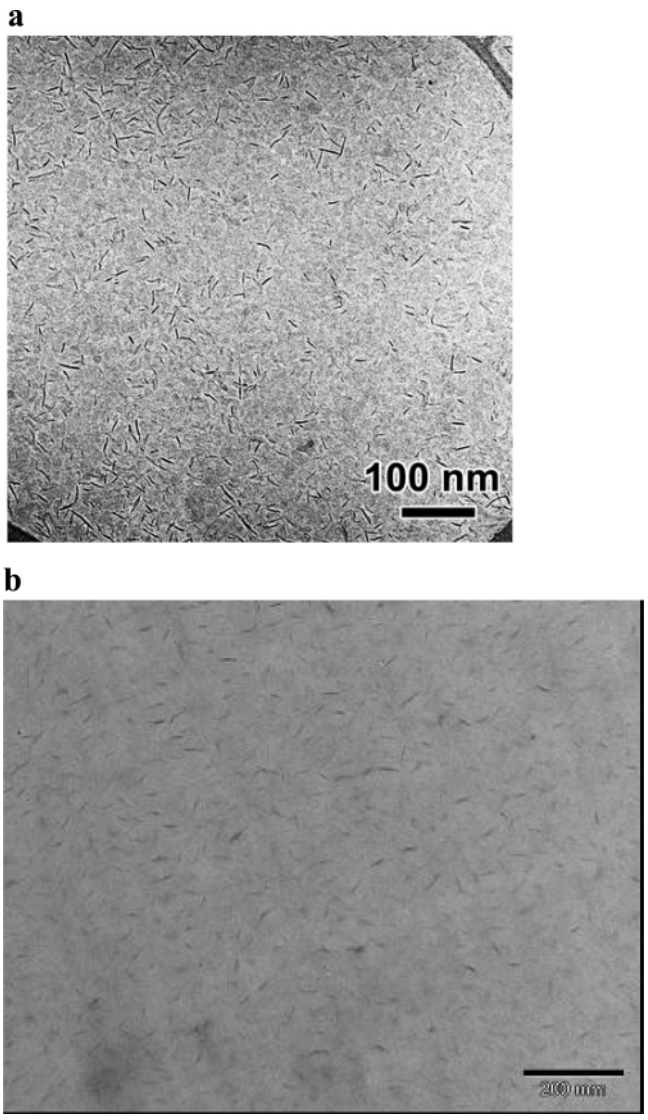

Figure 8. TEM images of (a) raw Laponite and (b) polystyrene-functionalized Laponite cast from a diluted toluene suspension. M_n of free PS = 55000 g/mol (sample 5 in Table 2).

is not optimal. Indeed, in an ideal controlled radical polymerization, PDI remains initially high before the establishement of the persistant radical effect and decreases with increasing conversion. The fact that in our case the PDI is high all long during polymerization suggests a poor efficiency of the alkoxyamine initiator. It is possible that the scavenging efficiency of DEPN is decreased consequently to the adsorption of DEPN moieties to the clay edges as discused previously. It is noteworthy to mention that similar PDI values and adsorption issues were already reported in previous papers on the graft polymerization of styrene from silica gel.[43,45] The further increase of PDI observed at higher conversions (e.g., 75%) could be attributed to the increase of the viscosity of the media with increasing conversion.

From the weight loss and the M_n of PS, we can estimate the polymer chains density and compare it to the density of initiator groups. The data in Table 2 indicate a surface polymer concentration in the range 100−180 mmol/100 g, which is up to 2 times higher than the initiator concentration. Although we took care to remove the free polymer by dialysis, the discrepancy between the number of intercalated initiator molecules and the number of polymer chains suggests the presence of physisorbed polymer on the clay surface. We have plotted in Figure 6 the evolution of the amount of surface polymer as monitored by TGA as a function of the polymer chains molecular weight. The data are compared to the theoretical values assuming 100% initiation efficiency. It is worth noticing that the two curves follow the same trend: the amount of surface polymer increases with increasing the polymer molecular weight as expected for a controlled polymerization. However, as stated previously, the amount of polymer binding is higher than the theoretical values. In addition, it is also noticeable that the difference between the experimental and the theoretical data is more important for low polymer molecular weights, e.g., for low reaction times. This suggests that if the extra organic content is indeed attributable to physisorption of the free polymer chains, the lower is the PS chain length, the more important is the adsorption. As mentioned above for the alkoxyamine initiator, adsorption can reasonably occur through hydrogen bonding between the end groups of the free polymer and the silanols located at the broken edges of the clay platelets. The higher is the polymer chain length, the better is its affinity for the solvant and the lower is consequently the adsorption on the clay surface. Although this is consistent with the experimental results, further investigations would be nevertheless required to confirm this scenario. It can be envisaged for instance to carry out the polymerization in the absence of sacrificial initiator in order to avoid the formation of free polymer and produce ionically bonded polystyrene chains only. This will be the subject of a future work. Indeed, the question of initiator efficiency under such heterogeneous conditions is an important issue which is still subject to debate. For instance, Wheeler and coauthors[24b] demonstrated that the ATRP of MMA initiated from the surface of Laponite platelets produced a number of chains equivalent to the number of initiating groups, whereas Billon et al. showed that only 35−45% of the initiator present on the surface of mica could initiate the growth of poly(*n*-butyl acrylate) chains by NMP.[44] At last, Sogah et al. have also estimated the initiation efficiency of a silicate anchored photoiniferter and showed that it was limited to around 25%, which was ascribed to initiator confinement in the clay galleries.[29]

Morphological Characterizations. Insights into the composite particles size and morphology were provided by DLS measurements and TEM analysis. While raw and alkoxyamine-intercalated Laponite particles formed aggregates and settled down in toluene, clay particles covered with polystyrene chains of molecular weights comprised between 9000 and 55 000 g mol^{-1}, formed stable colloidal suspensions with a mean diameter comprised between 80 and 127 nm (Table 1 and Figure 7). These suspensions are disturbed neither with time nor with centrifugation (15 000 rpm for 25 min), indicating that they are well stabilized. Figure 7 shows the evolution of the PS-grafted Laponite particles size as a function of the polystyrene molecular weight. The particles diameter first decreased and then increased with increasing the polystyrene chain length. This result suggests that for low polymer molecular weights the clay suspension still contains remaining clay aggregates. These aggregates are progressively destroyed upon increasing the polymer chain length as attested by the decrease in particles size. For higher polymer molecular weights, the particle size increases as the polymer chain length increases as expected for a graft polymerization. Figure 7b illustrates the extent of dispersion of PS-grafted Laponite with increasing molecular weights of the grafted polymer chains in THF. The bluish aspect of the suspensions indicates that clay aggregation is small relative to the wavelengths of visible light, and hence little diffraction occurs. For higher polymer molecular weights, the suspension

turns even more transparent with nearly no diffraction of light. It can be thus theorized that the intercalated polymer chains reduce the attractive forces between the clay layers and promote clay dispersion.

In addition, it is worth pointing out that the PS-grafted Laponites are readily dispersible into styrene, methyl methacrylate, butyl acrylate, acrylonitrile, or acrylamide, indicating that they are compatible with both nonpolar and polar monomers. This allows their potential utilization in miniemulsion polymerization, which process can be advantageously used to synthesize waterborne suspensions of polymer/inorganic composite colloids as demonstrated in a recent work from our group on the encapsulation of silica particles using this technique.[45] Figure 8 shows the TEM images of a thin cross section of a nanocomposite film cast from a 15 wt % toluene suspension. The Laponite platelets appear as dark rods regularly distributed within the polystyrene film (gray background) which definitely confirms that the clay is well-dispersed and completely exfoliated within the polymer matrix. Further evidence was provided by XRD analysis of the film which showed the absence of Bragg diffraction consequently to the complete loss of organization of the clay layers.

Conclusions

A novel quaternary ammonium alkoxyamine initiator was synthesized and intercalated into Na^+−Laponite through cation exchange. FTIR, XRD, and elemental analysis confirmed the presence of the initiator molecule in the clay galeries. An optimum amount of 72 mequiv/100 g corresponding to nearly full exchange of the cationic sites was obtained after washing for initial alkoxyamine concentrations corresponding to around 270% the CEC of Laponite. NMP of styrene initiated from the surface of the functionalized clay platelets displayed a living character, thus providing well-defined ionically bonded PS chains with molecular weights comprised between 9000 and 55 000 g/mol^{-1}. It was found that the grafting density of the surface-tethered PS chains quantified by TGA was higher than the amount of intercaled initiator, suggesting the presence of physisorbed polymer chains that could not be removed from the clay even after an exhaustive dialysis procedure. Adsorption was presumed to occur through hydrogen bonding between the end groups of the free polymer chains and the hydroxyls located at the edges of the clay platelets. At last, DLS measurements showed that the PS-functionalized Laponite displayed a remarkable high stability and dispersibility in organic solvent as well as into polar and nonpolar monomers. The PS chains formed on the clay surface promoted exfoliation of the clay tactoids by gradually pushing the clay layers appart during the growth reaction. The grafted PS chains thus created a steric barrier around the clay platelets which enabled to keep them dispersed in organic media. Films elaborated from these organic suspensions contained fully exfoliated Laponite platelets, indicating that the particles have retained their dispersability upon casting.

Acknowledgment. The authors are very grateful to Pierre Alcouffe (Laboratoire des Matériaux Polymère et Biomatériaux) for performing TEM analysis.

References and Notes

(1) (a) Kojima, Y.; Usuki, A.; Kawasumi, M.; Okada, A.; Kurauchi, T.; Kamigaito, O. *J. Polym. Sci., Part A: Polym. Chem.* **1993**, *31*, 983−986. (b) Usuki, A.; Kawasumi, M.; Kojima, Y.; Okada, A.; Kurauchi, T.; Kamigaito, O. *J. Mater. Res.* **1993**, *8*, 1174−1185.
(2) For reviews in this field, see: (a) Lagaly, G. *Appl. Clay Sci.* **1999**, *15*, 1−9. (b) Alexandre, M.; Dubois, P. *Mater Sci. Eng. Rep.* **2000**, *28*, 1−63. (c) Ray, S. S.; Okamoto, M. *Prog. Polym. Sci.* **2003**, *28*, 1539−1641.
(3) Song, K.; Sandi, G. *Clays Clay Mineral.* **2001**, *49*, 119−125.
(4) Negrete-Herrera, N.; Letoffe, J.-M.; Reymond, J.-P.; Bourgeat-Lami, E. *J. Mater. Chem.* **2005**, *15*, 863−871.
(5) Wheeler, P. A.; Wang, J.; Baker, J.; Mathis, L. J. *Chem. Mater.* **2005**, *17*, 3012−3018.
(6) Van Olphen, H. *An Introduction to Clay Colloid Chemistry*; Wiley-Interscience: New York, 1977.
(7) (a) Zeng, C.; Lee, L. J. *Macromolecules* **2001**, *34*, 4098−4103. (b) Fu, X.; Qutubuddin, S. *Polymer* **2001**, *42*, 807−813.
(8) (a) Fan, X.; Xia, C.; Advincula, R. C. *Langmuir* **2003**, *19*, 4381−4389. (b) Uthirakumar, P.; Kim, C.-J.; Nahm, K. S.; Hahn, Y. B.; Lee, Y.-S. *Colloids Surf., A* **2004**, *247*, 69−75. (c) Su, S.; Jiang, D. D.; Wilkie, C. A. *Polym. Adv. Technol.* **2004**, *15*, 225−231. (d) Fan, X.; Xia, C.; Advincula, R. C. *Langmuir* **2005**, *21*, 2537−2544.
(9) (a) Zhou, Q.; Fan, X.; Xia, C.; Mays, J.; Advincula, R. C. *Chem. Mater.* **2001**, *13*, 2465−2467. (b) Quirck, P.; Mathers, R. T. *Polym. Bull. (Berlin)* **2001**, *45*, 471−477. (c) Fan, X.; Zhou, Q.; Xia, C.; Cristofoli, W.; Mays, J.; Advincula, R. C. *Langmuir* **2002**, *18*, 4511−4518.
(10) Tsubokawa, N.; Kimoto, T.; Endo, T. *Polym. Bull. (Berlin)* **1994**, *33*, 187−194.
(11) Lepoittevin, B.; Pantoustier, N.; Devalckenaere, M.; Alexandre, M.; Kubies, D.; Calberg, C.; Jérôme, R.; Dubois, P. *Macromolecules* **2002**, *35*, 8385−8390.
(12) Hawker, C. J.; Barclay, G. G.; Orellana, A.; Dao, J.; Devonport, W. *Macromolecules* **1996**, *29*, 5245−5254.
(13) (a) Ejaz, M.; Yamamoto, S.; Ohno, K.; Tsujii, Y.; Fukuda, T. *Macromolecules* **1998**, *31*, 5934−5936. (b) Huang, X.; Doneski, L. J.; Wirth, M. J. *Anal. Chem.* **1998**, *70*, 4023−4029. (c) Husseman, M.; Malmström, E. E.; McNamara, M.; Mate, M.; Mecerreyes, D.; Benoit, D.; Hedrick, J. L.; Mansky, P.; Huang, E.; Russel, T. P.; Hawker, C. J. *Macromolecules* **1999**, *32*, 1424−1431. (d) Devaux, C.; Beyou, E.; Chapel, J. P.; Chaumont, P. *Eur. Phys. J.* **2002**, *7*, 345−352. (e) Baum, M.; Brittain, W. J. *Macromolecules* **2002**, *35*, 610−615. (f) Tomlinson, M. R.; Genzer, J. *Macromolecules* **2003**, *36*, 3449−3451.
(14) (a) von Werne, T.; Patten, T. E. *J. Am. Chem. Soc.* **1999**, *121*, 7409−7410. (b) Böttcher, H.; Hallensleben, M. L.; Nuss, S.; Wurm, H. *Polym. Bull. (Berlin)* **2000**, *44*, 223−229. (c) von Werne, T.; Patten, T. E. *J. Am. Chem. Soc.* **2001**, *123*, 7497−7505. (d) Blomberg, S.; Ostberg, S.; Harth, E.; Bosman, A. W.; van Horn, B.; Hawker, C. J. *J. Polym. Sci., Part A: Polym. Chem.* **2002**, *40*, 1309−1320. (e) Matsuno, R.; Yamamoto, K.; Otsuka, H.; Takahara, A. *Chem. Mater.* **2003**, *15*, 3−5. (f) Bartholome, C.; Beyou, E.; Bourgeat-Lami, E.; Chaumont, P.; Zydowicz, N. *Macromolecules* **2003**, *36*, 7946−7952. (g) Pyun, J.; Kowalewski, T.; Matyjaszewski, K. *Macromol. Rapid Commun.* **2003**, *24*, 1043−1059. (h) Matsuno, R.; Yamamoto, K.; Otsuka, H.; Takahara, A. *Macromolecules* **2004**, *37*, 2203−2209. (i) Parvole, J.; Laruelle, G.; Guimon, C.; François, J.; Billon, L. *Macromol. Rapid Commun.* **2003**, *24*, 1074−1078. (j) Laruelle, G.; Parvole, J.; François, J.; Billon, L. *Polymer* **2004**, *45*, 5013−5020. (k) Parvole, J.; Billon, L.; Montfort, J. P. *Polym. Int.* **2002**, *51*, 1111−1116. (l) Kasseh, A.; Ait-Kadi, A.; Riedl, B.; Pierson, J. F. *Polymer* **2003**, *44*, 1367−1375. (m) Ohno, K.; Morinaga, T.; Koh, K.; Tsujii, Y.; Fukuda, T. *Macromolecules* **2005**, *38*, 2137−2142. (n) Li, C.; Han, J.; Ryu, C. Y.; Benicewicz, B. C. *Macromolecules* **2006**, *39*, 3175−3183.
(15) Gu, B.; Sen, A. *Macromolecules* **2002**, *35*, 8913−8916.
(16) Wang, Y.; Teng, X.; Wang, J. S.; Yang, H. *Nano Lett.* **2003**, *3*, 789−793.
(17) Farmer, S. C.; Patten, T. E. *Chem. Mater.* **2001**, *13*, 3920−3926.
(18) (a) Tsujii, Y.; Ejaz, M.; Sato, K.; Goto, A.; Fukuda, T. *Macromolecules* **2001**, *34*, 8872−8878. (b) Nuss, S.; Böttcher, H.; Wurm, H.; Hallensleben, M. L. *Angew. Chem., Int. Ed.* **2001**, *40*, 4016−4018. (c) Ohno, K.; Koh, K.; Tsujji, Y.; Fukuda, T. *Macromolecules* **2002**, *35*, 8989−8993.
(19) Weimer, M. W.; Chen, H.; Giannelis, E. P.; Sogah, D. Y. *J. Am. Chem. Soc.* **1999**, *121*, 1615−1616.
(20) Di, J.; Sogah, D. Y. *Macromolecules* **2006**, *39*, 5052−5057.
(21) Böttcher, H.; Hallensleben, M. L.; Nuss, S.; Wurm, H.; Bauer, J.; Behrens, P. *J. Mater. Chem.* **2002**, *12*, 1351−1354.
(22) Zhao, H. Y.; Argoti, S. D.; Farrell, B. P.; Shipp, D. A. *J. Polym. Sci., Polym. Chem.* **2004**, *42*, 916−924.
(23) Li, C.-P.; Huang, C.-M.; Hsieh, M.-T.; Wei, K.-H. *J. Polym. Sci., Polym. Chem.* **2005**, *43*, 534−542.
(24) (a) Wheeler, P.; Mathias, L. *Macromol. Synth.* **2004**, *13*, 1. (b) Wheeler, P. A.; Wang, J.; Mathias, L. J. *Chem. Mater.* **2006**, *18*, 3937−3945.
(25) Zhao, H. Y.; Farrell, B. P.; Shipp, D. A. *Chem. Mater.* **2003**, *15*, 2693−2695.
(26) Zhao, H. Y.; Farrell, B. P.; Shipp, D. A. *Polymer* **2004**, *45*, 4473−4481.
(27) Salem, N.; Shipp, D. A. *Polymer* **2005**, *46*, 8573−8581.
(28) Zhang, B.-Q.; Pan, C.-Y.; Hong, C.-Y.; Luan, B.; Shi, P.-J. *Macromol. Rapid Commun.* **2006**, *27*, 97−102.
(29) Di, J.; Sogah, D. Y. *Macromolecules* **2006**, *39*, 1020−1028.

(30) Couturier, J. L.; Guerret, O. WO 0212149, 2002.
(31) Dao, J.; Benoit, D.; Hawker, C. J. *J. Polym. Sci.* **1998**, *36*, 2161−2167.
(32) The alkoxyamine was water soluble up to a concentration of 18 g L^{-1} and required about 1 h to fully dissolve.
(33) Koppel, D. J. *Chem. Phys.* **1972**, *57*, 4814−4820.
(34) (a) Yui, T.; Yoshida, H.; Tachibana, H.; Tryk, D. A.; Inoue, H. *Langmuir* **2002**, *18*, 891. (b) Török, B.; Balazsik, K.; Dekany, I.; Bartok, M. *Mol. Cryst.* **2000**, *341*, 339. (c) Ramsey, J. D. F.; Lindner, P. *J. Chem. Soc., Faraday Trans.* **1993**, *89*, 4207. (d) Mourchid, A.; Delville, A.; Levitz, P. *Faraday Discuss.* **1995**, *101*, 275.
(35) Levitz, P.; Lecolier, E.; Mourchid, A.; Delville, A.; Lyonnard, S. *Europhys. Lett.* **2000**, *49*, 672−677.
(36) Patzko, A.; Dekany, I. *Colloids Surf., A* **1993**, *71*, 299−307.
(37) Connolly, J.; van Duijneveldt, J. S.; Klein, S.; Pizzey, C.; Richardson, R. M. *Langmuir* **2006**, *22*, 6531−6538.
(38) Greenland, D. J.; Quirk, J. P. *Clays Clay Mineral.* **1962**, *9*, 484.
(39) Röhl, W.; Rybinsky, W.; Schwuger, M. J. *Prog. Colloid Polym. Sci.* **1991**, *84*, 206.
(40) Brahimi, B.; Labbe, P.; Reverdy, G. *Langmuir* **1992**, *8*, 1908−1918.
(41) Kubies, D.; Jérôme, R.; Grandjean, J. *Langmuir* **2002**, *18*, 6159−6163.
(42) Zhang, Z. Z.; Sparks, D. L.; Scrivner, N. C. *Environ. Sci. Technol.* **1993**, *27*, 1625.
(43) Bartholome, C.; Beyou, E.; Bourgeat-Lami, E.; Chaumont, P.; Lefebvre, F.; Zydowicz, N. *Macromolecules* **2005**, *38*, 1099−1036.
(44) Ghannam, L.; Bacou, M.; Garay, H.; Shanahan, M. E. R.; François, J.; Billon, L. *Polymer* **2004**, *45*, 7035−7045.
(45) Bartholome, C.; Beyou, E.; Bourgeat-Lami, E.; Chaumont, P. *J. Nanomater.* **2006**, *2006*, 1−10.

MA070283G